

## Isospin symmetry and proton decay: Identification of the $10^+$ isomer in $^{54}\text{Ni}$

D. Rudolph,<sup>1</sup> R. Hoischen,<sup>1,2</sup> M. Hellström,<sup>1</sup> S. Pietri,<sup>3</sup> Zs. Podolyák,<sup>3</sup> P. H. Regan,<sup>3</sup> A. B. Garnsworthy,<sup>3,4</sup> S. J. Steer,<sup>3</sup> F. Becker,<sup>2,\*</sup> P. Bednarczyk,<sup>2,5</sup> L. Cáceres,<sup>2,6</sup> P. Doornenbal,<sup>2,7,†</sup> J. Gerl,<sup>2</sup> M. Górska,<sup>2</sup> J. Grębosz,<sup>2,5</sup> I. Kojouharov,<sup>2</sup> N. Kurz,<sup>2</sup> W. Prokopowicz,<sup>2,5</sup> H. Schaffner,<sup>2</sup> H. J. Wollersheim,<sup>2</sup> L.-L. Andersson,<sup>1</sup> L. Atanasova,<sup>8</sup> D. L. Balabanski,<sup>8,9</sup> M. A. Bentley,<sup>10</sup> A. Blazhev,<sup>7</sup> C. Brandau,<sup>2,3</sup> J. R. Brown,<sup>10</sup> C. Fahlander,<sup>1</sup> E. K. Johansson,<sup>1</sup> A. Jungclauss,<sup>6</sup> and S. M. Lenzi<sup>11</sup>

<sup>1</sup>Department of Physics, Lund University, S-22100 Lund, Sweden

<sup>2</sup>Gesellschaft für Schwerionenforschung mbH, D-64291 Darmstadt, Germany

<sup>3</sup>Department of Physics, University of Surrey, Guildford, GU2 7XH, United Kingdom

<sup>4</sup>Wright Nuclear Structure Laboratory, Yale University, New Haven, Connecticut 06520-8124, USA

<sup>5</sup>The Henryk Niewodniczanski Institute of Nuclear Physics (IFJ PAN), PL-31342 Kraków, Poland

<sup>6</sup>Departamento de Física Teórica, Universidad Autónoma de Madrid, E-28049 Madrid, Spain

<sup>7</sup>Institut für Kernphysik, Universität zu Köln, D-50937 Köln, Germany

<sup>8</sup>Faculty of Physics, University of Sofia, BG-1164 Sofia, Bulgaria

<sup>9</sup>Bulgarian Academy of Sciences, BG-1784 Sofia, Bulgaria

<sup>10</sup>Department of Physics, University of York, York, YO10 5DD, United Kingdom,

<sup>11</sup>Dipartimento di Fisica dell'Università and INFN, Sezione di Padova, I-35131 Padova, Italy

(Received 7 February 2008; published 6 August 2008)

The  $\gamma$  decays from an isomeric  $10^+$  state at 6457 keV in the nucleus  $^{54}_{28}\text{Ni}_{26}$  have been identified using the GSI fragment separator in conjunction with the RISING Ge-detector array. The state is interpreted as the isobaric analog of the 6527-keV  $10^+$  isomer in  $^{54}_{26}\text{Fe}_{28}$ . The results are discussed in terms of isospin-dependent shell-model calculations. Clear evidence is presented for a discrete  $\ell = 5$  proton decay branch into the first excited  $9/2^-$  state of the daughter  $^{53}\text{Co}$ . This decay is the first of its kind observed following projectile fragmentation reactions.

DOI: [10.1103/PhysRevC.78.021301](https://doi.org/10.1103/PhysRevC.78.021301)

PACS number(s): 23.20.-g, 23.50.+z, 25.70.Mn, 27.40.+z

A central topic in contemporary nuclear structure physics is the investigation of exotic nuclear matter far from the line of  $\beta$  stability. Long-standing questions are “Where are the proton and neutron drip lines situated?” and “How does the nuclear force depend on varying proton-to-neutron ratios?” [1]. These issues can be addressed by investigating long isotopic chains: The magic  $Z = 28$  nickel chain covers four potentially doubly-magic nuclides, namely, with  $N = 20$ ,  $N = 28$ ,  $N = 40$ , and  $N = 50$ . Indeed,  $^{48}\text{Ni}$  is found to denote the proton dripline [2], while measurements on  $^{78}\text{Ni}$  provide crucial information on the astrophysical rapid neutron capture process [3]. As with  $^{68}\text{Ni}$  [4], the self-conjugate  $N = Z$  nucleus  $^{56}\text{Ni}$  shows distinct features of a soft doubly-magic core, becoming strongly deformed at modest excitation energies and angular momenta. Furthermore, a rotational state at  $\sim 10$  MeV excitation energy in  $^{56}\text{Ni}$  revealed a fast, discrete proton decay branch [5,6].

Another evergreen of nuclear structure studies along the  $N = Z$  line is isospin symmetry or, more precisely, the breaking of isospin symmetry due to the Coulomb force as well as, possibly, some components of the strong nucleon-nucleon interaction [7]. Here, the so-called “ $J = 2$  anomaly” must be mentioned: It relates to unusual mirror energy differences (MED) in excited states, the wave functions of which are thought to be dominated by spin  $J = 2$ , isospin  $T = 1$  couplings [7–9]. During the past decade, the prime region for such investigations has been the rather well-confined  $\mathcal{N} = 3$ ,

“ $fp$  shell” reaching from  $^{40}\text{Ca}$  toward  $^{80}\text{Zr}$  while passing  $^{56}\text{Ni}$ . Related work has been summarized recently [10–12].

This rapid communication provides new experimental results on the  $T_z = -1$  nucleus  $^{54}\text{Ni}$ , hence addressing both the dripline and the isospin symmetry breaking aspects indicated above. The existence of an isomeric  $10^+$  state in  $^{54}\text{Fe}$  has been known for decades [13], and thus an isobaric analog state is expected to exist in  $^{54}\text{Ni}$ . Besides basic studies of MED, its observation bears the potential of isospin symmetry studies of electromagnetic moments and decay properties, for example, an independent check on the recently established isoscalar and isovector polarization charges near  $^{56}\text{Ni}$  [14] and a possible extension to  $E4$  transitions. Previous knowledge on  $^{54}\text{Ni}$  includes the yrast  $6^+ \rightarrow 4^+ \rightarrow 2^+ \rightarrow 0^+$  ground-state cascade established via in-beam  $\gamma$ -ray spectroscopy [9] and measurements of  $B(E2; 2^+ \rightarrow 0^+) = 122(24) e^2\text{fm}^4$  by relativistic Coulomb excitation experiments [15,16].

Within the *Rare Isotope Spectroscopic INvestigations at GSI* (RISING) campaign, the nuclei of interest were produced by fragmentation of a  $^{58}\text{Ni}$  primary beam at 550 MeV/u on a  $1 \text{ g/cm}^2$   $^9\text{Be}$  target. Subsequently, the reaction products were selected by means of a  $B\rho - \Delta E - B\rho$  technique in the *FRAGMENT SEPARATOR* (FRS) [17]. The ion-by-ion identification in terms of mass,  $A$ , and proton number,  $Z$ , of each transmitted ion is performed uniquely with a suite of scintillator and ionization detectors placed at the intermediate and final focus of the FRS. The identified secondary ions, namely,  $^{51,52}\text{Fe}$  (0.4%),  $^{52,53}\text{Co}$  (15.5 and 21.3%), and  $^{53,54,55}\text{Ni}$  (1.4, 58.6, and 2.8%), finally came to rest in a 4 mm thick Be plate after some 350 ns flight time through the FRS. The Be plate was

\*Present address: FZ Karlsruhe

†Present address: RIKEN

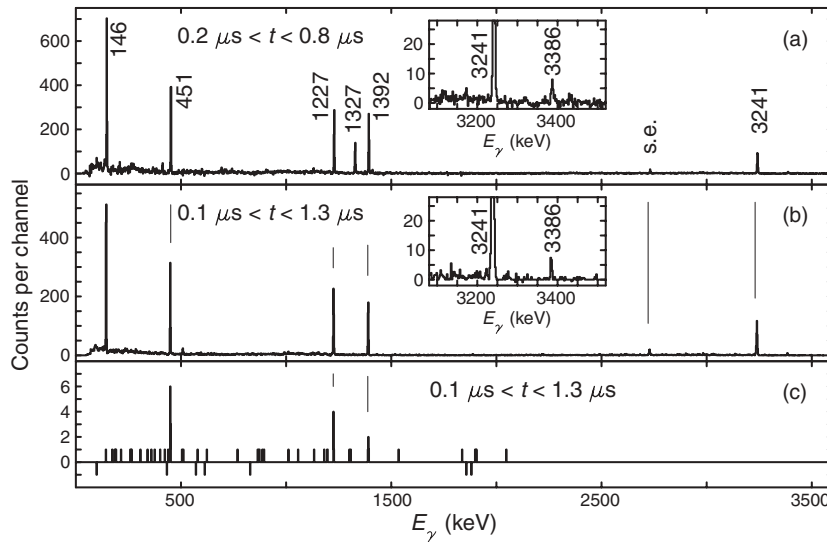


FIG. 1.  $\gamma$ -ray spectra associated with implanted  $^{54}\text{Ni}$  ions. Part (a) shows a spectrum requiring a complete ion identification. It was taken between 0.2 and 0.8  $\mu\text{s}$  after implantation. Implantation-correlated background radiation is removed with correspondingly selected spectra of other implanted ions, namely,  $^{53,55}\text{Ni}$  and  $^{52,53}\text{Co}$ , which do not show any delayed  $\gamma$  rays in this time range. Room and long-lived  $\beta$ -decay background is subtracted with a spectrum taken between 19.0 and 19.6  $\mu\text{s}$  after implantation. Parts (b) and (c) provide spectra in coincidence with the known yrast cascade [9] in  $^{54}\text{Ni}$  and the new 3386-keV,  $10^+ \rightarrow 6^+$   $E4$  transition.

surrounded by fifteen high-efficiency CLUSTER Ge detectors [18] for  $\gamma$ -ray detection. Each ion arriving at the final focus started a clock and subsequent  $\gamma$  decays from isomeric states were recorded for 20  $\mu\text{s}$  before the data acquisition system reset itself. More details on the experiment and the RISING setup can be found in Refs. [19,20].

During 60 h of beam time and employing a very restrictive and stringent heavy-ion identification procedure on the FRS data, some 4.8 million implanted  $^{54}\text{Ni}$  nuclei have been identified. Figure 1(a) provides the associated time-correlated and background subtracted  $\gamma$ -ray spectrum. It reveals seven delayed  $\gamma$ -ray transitions at 146.1(2), 451.0(3), 1227.4(4), 1327.3(4), 1392.3(4), 3240.7(7), and 3386.2(9) keV. The latter is highlighted in the inset, and the single-escape line of the 3241 keV transition is also present. The 451-, 1227-, and 1392-keV lines are known to belong to  $^{54}\text{Ni}$  [9]. The 146- and 3241-keV transitions are very similar in energy to the  $10^+ \rightarrow 8^+ \rightarrow 6^+$  sequence in the mirror nucleus  $^{54}\text{Fe}$ , and the 3386-keV line represents a parallel 5.1(11)%  $10^+ \rightarrow 6^+$   $E4$  branch. The branching ratio is corrected for possible pileup of the 146- and 3241-keV transitions in the same Ge detector. This scheme is underpinned by the  $\gamma$ -ray spectra in Figs. 1(b) and 1(c), which are based on delayed  $\gamma\gamma$  coincidences. Both the time range and the FRS identification scheme are somewhat relaxed to allow for increased statistics. The spectrum in Fig. 1(b) is taken in prompt coincidence with the known ground-state cascade and confirms the placement of the 146-, 3241-, and 3386-keV transitions on top of it. Figure 1(c) is the coincidence spectrum of the weak 3386-keV line, proving that it lies parallel to the 146- to 3241-keV cascade.

The peak at 1327 keV, which is clearly seen in Fig. 1(a), is absent in both Figs. 1(b) and 1(c); i.e., it is *not* in coincidence with any other  $\gamma$ -ray transition associated with the decay of the presumed  $10^+$  isomer in  $^{54}\text{Ni}$ . Nevertheless, within uncertainties the 1327-keV line exhibits the same half-life as the  $^{54}\text{Ni}$  transitions. This is shown in Fig. 2, which provides three scaled decay curves of the previously reported transitions in  $^{54}\text{Ni}$  (top), the new high-energetic ones (middle), and the 1327-keV line (bottom). The conclusion is that the single  $\gamma$  ray at 1327 keV must have the same isomeric origin as the

other six transitions. Because 1327 keV matches exactly the prompt  $9/2^- \rightarrow 7/2^-$  ground-state  $\gamma$  transition in  $^{53}\text{Co}$  [8], a discrete 1.28(5)-MeV,  $\ell = 5$  proton decay from the isomeric  $10^+$  state in  $^{54}\text{Ni}$  into the excited  $9/2^-$  state in the daughter  $^{53}\text{Co}$  is inferred. This marks the first evidence for discrete proton emission competing with  $\gamma$  radiation following a projectile fragmentation reaction. The evidence is indirect, because both the present setup and the implantation depth of  $^{54}\text{Ni}$  ions in the stopper together with the short half-life prevent a direct measurement of the protons. Historically, this observation takes proton decay studies back to its roots, as the first reported proton decay ever was observed from the long-lived  $19/2^-$  high-spin state in  $^{53}\text{Co}$  [21,22]. The existence of the present type of discrete proton decay opens a plethora of subsequent, unprecedented investigations: isospin aspects of static moments and, ultimately, proton angular distributions from an aligned state with known quadrupole moment.

The lifetime of the  $10^+$  state in  $^{54}\text{Ni}$  averages to  $T_{1/2} = 152(4)$  ns. The experimental information is summarized in Table I and illustrated in Fig. 3.

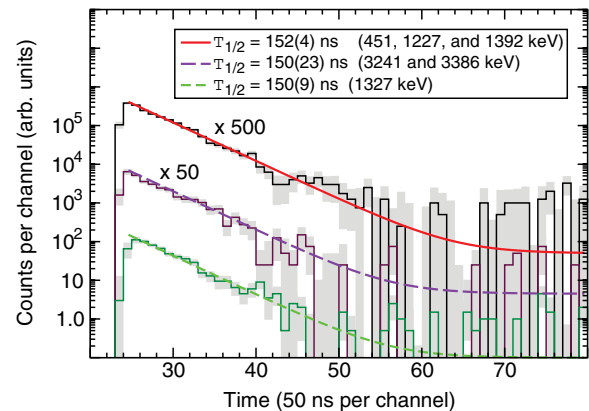


FIG. 2. (Color online) Decay curves of different combinations of  $\gamma$ -ray transitions associated with the isomeric  $10^+$  state in  $^{54}\text{Ni}$ . The lines represent the least-squares fits to the data.

TABLE I. Experimental results and theoretical predictions from isospin-dependent  $fp$  shell-model calculations. The experimental numbers of  $^{54}\text{Ni}$  are corrected for the measured 36(2)% proton branch.  $B(E2)$  and  $B(E4)$  values are in W.u.

Observable	$^{54}\text{Fe}$		$^{54}\text{Ni}$		
	exp [13]	KB3G	exp	KB3G	exp <sup>a</sup>
$B(E2; 6^+ \rightarrow 4^+)$	3.25(5)	2.85	–	2.29	–
$B(E2; 10^+ \rightarrow 8^+)^b$	1.69(4)	2.03	2.48(7)	2.06	1.98(6)
$B(E4; 10^+ \rightarrow 6^+)$	0.79(8)	1.30	5.7(13)	4.66	4.6(10)
$\text{br}_{\gamma+e^-}(10^+ \rightarrow 6^+)$	1.8(2)	2.4	5.1(11)	5.0	5.1(11)
$T_{1/2}(10^+)_{\gamma+e^-}$ (ns)	364(7)	303	237(6)	286	296(8)
$Q(10^+)$ ( $e\text{fm}^2$ )	52(8) <sup>c</sup>	55.6	–	58.5	–
$\mu(10^+)(\mu_N)$	7.281(10)	6.82	–	4.24	–

<sup>a</sup>Assuming an additional proton-decay branch,  $\text{br}_{p2}$ , into the ground state of  $^{53}\text{Co}$  with  $\text{br}_{\gamma+e^-} : \text{br}_{p1} : \text{br}_{p2} = 64(2) : 36(2) : 25$ .

<sup>b</sup>Including conversion coefficients of  $\alpha_{\text{tot}} = 0.115(4)$  and  $\alpha_{\text{tot}} = 0.135(4)$  for  $^{54}\text{Fe}$  and  $^{54}\text{Ni}$ , respectively [23].

<sup>c</sup>Using the revised  $Q(3/2^-)$  of  $^{57}\text{Fe}$  as outlined in Ref. [24].

Spherical large-scale shell-model calculations were performed with the code ANTOINE [25,26]. They employ the full  $fp$  space, but the model space needs to be truncated to allow for excitations of up to  $t = 6$  particles across the shell closure at  $N = Z = 28$ . This is a compromise between available computing power and sufficient convergence of the calculated numbers for near-spherical yrast states in the mass region [10–12,27]. The KB3G [28] and GXPF1A [29] interactions are studied, and for the main body of predictions isospin breaking terms are included.

Following the notations of Refs. [7,10,11], multipole harmonic-oscillator Coulomb matrix elements,  $V_{\text{CM}}$ , and the monopole electromagnetic spin-orbit effect,  $V_{\text{CIS}}$ , are readily

included. To account for other monopole related shifts of single-particle energy levels the prescription of Ref. [11] ( $V_{\text{Cr}}$ ) is followed. Finally, charge-asymmetric components of the strong nucleon-nucleon interaction are included. A repulsive 100-keV term,  $V_{BM-2}$ , was introduced for the  $1f_{7/2}^2$ ,  $J = 2$  two-proton matrix element by Zuker *et al.* [6] to account for an anomalous MED value of the  $2^+$  states in the  $A = 42$  mirror pair. The use of  $V_{BM-2}$  has been shown to improve the MED description of nuclei throughout the entire  $1f_{7/2}$  shell [8–10]. Electromagnetic decay properties are calculated with the  $E2$  effective charges of  $e_{\text{eff}}^p = 1.15$  and  $e_{\text{eff}}^n = 0.80$  derived in Ref. [14], while for  $B(E4)$  strengths the values [12]  $e_{\text{eff}}^p = 1.5$  and  $e_{\text{eff}}^n = 0.5$  are used as a starting point [30].

Figure 3 compares the energy levels of the KB3G interaction with the experimental cascade in  $^{54}\text{Ni}$  (and  $^{54}\text{Fe}$ ). The known  $1f_{7/2}^{-2}$  dominated  $0^+$ ,  $2^+$ ,  $4^+$ ,  $6^+$  yrast cascade [9] is well described. However, some deficiencies of the interaction become apparent for the core-excited  $8^+$  and  $10^+$  states: the energy gap is predicted somewhat too large, and the two states are inverted, though still within the typical predictive power for level energies [10,12].

Figure 4 provides the experimental MED diagram for the  $T_z = \pm 1$ ,  $A = 54$  system (black dots) and the predictions using the KB3G interaction. Though differing in details, predictions using the GXPF1A interaction do yield essentially the same picture. The calculations *without* any nuclear isospin breaking component (dotted line) fail to reproduce the MED of the  $2^+$  states. While this is expected [7,9], also the MED values of the  $8^+$  and  $10^+$  states are being missed. In turn, the MED predictions including  $V_{BM-2}$  (solid black line) are in nearly perfect agreement with the experimental values; i.e., they account for the above-mentioned MED discrepancies at *both* spin  $I = 2$  and spins  $I = 8$  and  $I = 10$ . A similar effect on MED values might be achieved by instead using an attractive 100-keV term,  $V_{BM-0}$ , for the  $1f_{7/2}^2$ ,  $J = 0$  two-proton matrix element. In fact, the calculation using the  $V_{BM-0}$  term (solid grey line) also improves on the MED of the  $2^+$ ,  $8^+$ , and  $10^+$  states. However, the predictions for the intermediate spin  $I = 4$

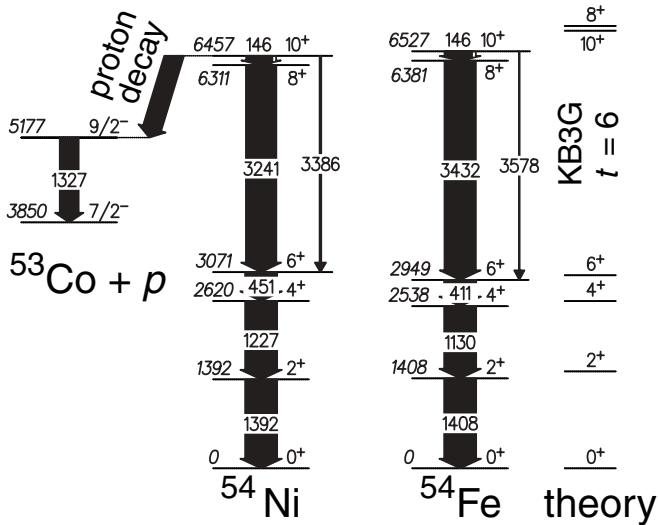


FIG. 3. Decay scheme of the  $10^+$  isomer in  $^{54}\text{Ni}$  deduced from the present work. The relevant decays of the mirror nucleus  $^{54}\text{Fe}$  [13] are shown for comparison. On the right-hand side, level energies from isospin-symmetric  $A = 54$ ,  $T = 1$  shell-model calculations are shown. See text for details.

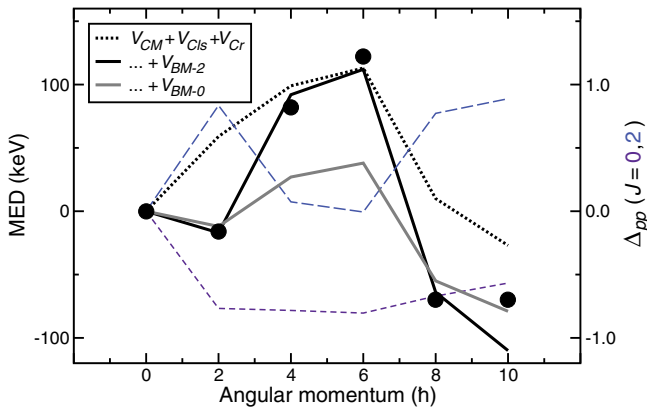


FIG. 4. (Color online) Mirror energy difference,  $E_x(^{54}\text{Ni}) - E_x(^{54}\text{Fe})$ , as a function of spin. Solid circles denote the experimental values. The dotted line accounts only for Coulomb related isospin breaking terms [11], while the solid black and grey lines include the  $V_{BM-2}$  [7] and  $V_{BM-0}$  terms, based on the KB3G interaction. The long- and short-dashed lines provide the difference between  $^{54}\text{Fe}$  and  $^{54}\text{Ni}$  of  $T = 1$  proton pairs,  $\Delta_{pp}$ , coupled to either  $J = 2$  or  $J = 0$ , respectively.

and  $I = 6$  states are significantly worsened; i.e.,  $V_{BM-0}$  seems to be able to improve the MED predictions locally, while  $V_{BM-2}$  appears to act globally.

To study the influence of these two nuclear isospin breaking terms in some more detail, Fig. 4 provides also the difference of the number of two-proton  $J = 0$  pairs [thin dashed lines,  $\Delta_{pp}(J = 0)$ ] and  $J = 2$  pairs [thin long-dashed lines,  $\Delta_{pp}(J = 2)$ ] between  $^{54}\text{Fe}$  and  $^{54}\text{Ni}$  as a function of angular momentum. In the case of  $\Delta_{pp}(J = 0)$ , the curve trivially drops exactly once between  $I = 0$  and  $I = 2$ , but then remains essentially constant. On the contrary,  $\Delta_{pp}(J = 2)$  peaks at  $I = 2$  and once more at  $I = 8$  and  $I = 10$ , which is nicely correlated with the respective global reproduction of the experimental MED with shell-model calculations accounting for the  $V_{BM-2}$  term. This presents the first clear evidence that the non-Coulomb isospin-breaking component has its origin in the  $J = 2$  coupling, rather than  $J = 0$ , of  $1f_{7/2}$  particles.

Experimental and predicted electromagnetic decay properties are compared in Table I. Excellent agreement is achieved, with two exceptions: the  $B(E4)$  strength in  $^{54}\text{Fe}$  and its related  $E4$  branch, and the lifetime of the isomer itself in  $^{54}\text{Ni}$ . The

latter discrepancy becomes more obvious when comparing the ratios of the lifetime predictions,  $R = 1.06$ , with the experimental values,  $R = 1.53(5)$ . This rather significant mismatch could be cured by an additional  $\sim 25\%$  proton branch into the ground state of  $^{53}\text{Co}$ , to which the present experiment is insensitive. The right-most column of Table I includes this correction. Indeed, simple WKB estimates provide similar tunneling probabilities for a 1.28-MeV,  $\ell = 5$  proton into the  $9/2^-$  state in  $^{53}\text{Co}$  and a 2.61-MeV,  $\ell = 7$  proton into the ground state of  $^{53}\text{Co}$  [31]; the structural hindrance factors are on the order of  $10^6$ , which remain to be explained by tiny  $1h_{11/2}$  or  $1j_{13/2}$  proton partitions in the wave function of the  $10^+$  state in  $^{54}\text{Ni}$ .

The possible existence of a second proton branch prevents a dedicated analysis of  $E4$  polarization charges along the scheme developed in Ref. [14], because an absolute number for the  $10^+ \rightarrow 6^+$  transition in  $^{54}\text{Ni}$  is missing. Nevertheless, using the extremes the ratio of the  $B(E4)$  values in  $^{54}\text{Fe}$  and  $^{54}\text{Ni}$  is limited to  $R \sim 0.10\text{--}0.25$ , which requires negative isovector  $E4$  polarization charges. The best agreement for the (corrected) experimental data is achieved with  $e_{\text{eff},p}(E4) \sim 1.35$  and  $e_{\text{eff},n}(E4) \sim 0.25$ .

In summary, the  $10^+$  mirror isomer in  $^{54}\text{Ni}$  has been identified. Its electromagnetic decay characteristics provide new constraints on large-scale  $fp$  shell-model calculations in conjunction with isospin symmetry. It is shown that the MED values for the  $2^+$ ,  $8^+$ , and  $10^+$  states can be associated with the isospin symmetry breaking  $J = 2$ ,  $T = 1$  interaction. Evidence is presented for a distinct direct proton decay branch into the excited  $9/2^-$  state in  $^{53}\text{Co}$ , and a significant discrepancy of the experimental and predicted half-life of the isomer points to an additional proton branch into the ground state of  $^{53}\text{Co}$ .

The authors gratefully acknowledge the outstanding work of the GSI accelerator and ion-source crews in providing the experiment with the envisaged high beam intensities. This work is supported by the European Commission (Contract 506065) (EURONS), the Swedish Research Council, the EPSRC (United Kingdom), the German BMBF, the Polish Ministry of Science and Higher Education, the Bulgarian Science Fund, the Spanish Ministerio de Educación y Ciencia, and the U.S. Department of Energy.

- [1] NuPECC Long Range Plan 2004, edited by M. Harakeh *et al.*, www.nupecc.org, (2004).  
 [2] C. Dossat *et al.*, Phys. Rev. C **72**, 054315 (2005).  
 [3] P. T. Hosmer *et al.*, Phys. Rev. Lett. **94**, 112501 (2005).  
 [4] O. Sorlin *et al.*, Phys. Rev. Lett. **88**, 092501 (2002).  
 [5] D. Rudolph *et al.*, Phys. Rev. Lett. **82**, 3763 (1999).  
 [6] E. K. Johansson *et al.*, Phys. Rev. C **77**, 064316 (2008).  
 [7] A. P. Zuker, S. M. Lenzi, G. Martinez-Pinedo, and A. Poves, Phys. Rev. Lett. **89**, 142502 (2002).  
 [8] S. J. Williams *et al.*, Phys. Rev. C **68**, 011301(R) (2003).  
 [9] A. Gadea *et al.*, Phys. Rev. Lett. **97**, 152501 (2006).  
 [10] M. A. Bentley and S. M. Lenzi, Prog. Part. Nucl. Phys. **59**, 497 (2007).  
 [11] J. Ekman, C. Fahlander, and D. Rudolph, Mod. Phys. Lett. A **20**, 2977 (2005).  
 [12] E. Caurier *et al.*, Rev. Mod. Phys. **77**, 427 (2005).  
 [13] H. Junde and H. Su, Nucl. Data Sheets **107**, 1393 (2006).  
 [14] R. du Rietz *et al.*, Phys. Rev. Lett. **93**, 222501 (2004).  
 [15] K. L. Yurkewicz *et al.*, Phys. Rev. C **70**, 054319 (2004).  
 [16] K. Yamada *et al.*, Eur. Phys. J. A **25** S1, 409 (2005).  
 [17] H. Geissel *et al.*, Nucl. Instrum. Methods B **70**, 286 (1992).  
 [18] J. Eberth *et al.*, Nucl. Instrum. Methods A **369**, 135 (1996).  
 [19] S. Pietri *et al.*, Acta Phys. Pol. **38**, 1255 (2007); Nucl. Instrum. Methods B **261**, 1079 (2007).

- [20] D. Rudolph *et al.*, *Eur. Phys. J. A* **36**, 131 (2008).
- [21] K. P. Jackson *et al.*, *Phys. Lett.* **B33**, 281 (1970).
- [22] J. Cerny *et al.*, *Phys. Lett.* **B33**, 284 (1970).
- [23] T. Kibédi *et al.*, *AIP Conf. Proc.* **769**, 268 (2005).
- [24] G. Martínez-Pinedo *et al.*, *Phys. Rev. Lett.* **87**, 062701 (2001).
- [25] E. Caurier, shell model code ANTOINE, IReS Strasbourg 1989, 2002.
- [26] E. Caurier and F. Nowacki, *Acta Phys. Pol.* **30**, 705 (1999).
- [27] M. Horoi, B. A. Brown, T. Otsuka, M. Honma, and T. Mizusaki, *Phys. Rev. C* **73**, 061305(R) (2006).
- [28] A. Poves *et al.*, *Nucl. Phys.* **A694**, 157 (2001).
- [29] M. Honma, T. Otsuka, B. A. Brown, and T. Mizusaki, *Phys. Rev. C* **65**, 061301(R) (2002); **69**, 034335 (2004); *Eur. Phys. J. A* **25**, s01, 499 (2005).
- [30] A. Gadea *et al.*, *Phys. Lett.* **B619**, 88 (2005).
- [31] S. Hofmann (private communication).